

P1 1105324

RECEIVED

19 DEC 2003

WIPO

PCT

THE UNITED STATES OF AMERICA

TO ALL TO WHOM THESE PRESENTS SHALL COME:

UNITED STATES DEPARTMENT OF COMMERCE
United States Patent and Trademark Office

December 16, 2003

THIS IS TO CERTIFY THAT ANNEXED HERETO IS A TRUE COPY FROM
THE RECORDS OF THE UNITED STATES PATENT AND TRADEMARK
OFFICE OF THOSE PAPERS OF THE BELOW IDENTIFIED PATENT
APPLICATION THAT MET THE REQUIREMENTS TO BE GRANTED A
FILING DATE.

APPLICATION NUMBER: 60/418,511

FILING DATE: October 15, 2002

RELATED PCT APPLICATION NUMBER: PCT/US03/32616



By Authority of the
COMMISSIONER OF PATENTS AND TRADEMARKS


M. K. HAWKINS
Certifying Officer

BEST AVAILABLE COPY

PRIORITY DOCUMENT
SUBMITTED OR TRANSMITTED IN
COMPLIANCE WITH
RULE 17.1(a) OR (b)

10-16-02

A/PROL

10/15/02

138 U.S. PRO


Under the Paperwork Reduction Act of 1995, no persons are required to respond to a collection of information unless it displays a valid OMB control number.
Approved for use through 10/31/2002. OMB 0851-0032
U.S. Patent and Trademark Office; U.S. DEPARTMENT OF COMMERCE

PROVISIONAL APPLICATION FOR PATENT COVER SHEET

This is a request for filing a PROVISIONAL APPLICATION FOR PATENT under 37 CFR 1.53(c).

Express Mail Label No. EL085174353US

138 U.S. PRO
08/418511

INVENTOR(S)					
Given Name (first and middle [if any])		Family Name or Surname		Residence (City and either State or Foreign Country)	
Cynthia		Roberts		1667 Moreland Drive Columbus, OH 43220 US	
<input checked="" type="checkbox"/> Additional inventors are being named on the <u>1</u> separately numbered sheets attached hereto					
TITLE OF THE INVENTION (500 characters max)					
Method and System for Designing an Improved Ablation Pattern					
Direct all correspondence to: CORRESPONDENCE ADDRESS					
<input checked="" type="checkbox"/> Customer Number				 Place Customer Number Bar Code Label Here 24024 PATENT TRADEMARK OFFICE	
OR Type Customer Number here					
<input type="checkbox"/> Firm or Individual Name					
Address					
Address					
City		State		ZIP	
Country		Telephone		Fax	
ENCLOSED APPLICATION PARTS (check all that apply)					
<input checked="" type="checkbox"/> Specification Number of Pages		27		<input type="checkbox"/> CD(s), Number	
<input checked="" type="checkbox"/> Drawing(s) Number of Sheets		18		<input type="checkbox"/> Other (specify)	
<input type="checkbox"/> Application Data Sheet. See 37 CFR 1.76					
METHOD OF PAYMENT OF FILING FEES FOR THIS PROVISIONAL APPLICATION FOR PATENT					
<input checked="" type="checkbox"/> Applicant claims small entity status. See 37 CFR 1.27.				FILING FEE AMOUNT (\$)	
<input checked="" type="checkbox"/> A check or money order is enclosed to cover the filing fees				80.00	
<input checked="" type="checkbox"/> The Commissioner is hereby authorized to charge filing fees or credit any overpayment to Deposit Account Number:		03-0172			
<input type="checkbox"/> Payment by credit card. Form PTO-2038 is attached.					
The invention was made by an agency of the United States Government or under a contract with an agency of the United States Government.					
<input checked="" type="checkbox"/> No.					
<input type="checkbox"/> Yes, the name of the U.S. Government agency and the Government contract number are:					

Respectfully submitted,

SIGNATURE 

TYPED or PRINTED NAME John T. Kalnay

TELEPHONE 216-622-8248

Date Oct-15, 02

REGISTRATION NO.
(If appropriate)
Docket Number:

46,816
18525-04063

USE ONLY FOR FILING A PROVISIONAL APPLICATION FOR PATENT

This collection of information is required by 37 CFR 1.51. The information is used by the public to file (and by the PTO to process) a provisional application. Confidentiality is governed by 35 U.S.C. 122 and 37 CFR 1.14. This collection is estimated to take 8 hours to complete, including gathering, preparing, and submitting the complete provisional application to the PTO. Time will vary depending upon the individual case. Any comments on the amount of time you require to complete this form and/or suggestions for reducing this burden, should be sent to the Chief Information Officer, U.S. Patent and Trademark Office, U.S. Department of Commerce, Washington, D.C. 20231. DO NOT SEND FEES OR COMPLETED FORMS TO THIS ADDRESS. SEND TO: Box Provisional Application, Assistant Commissioner for Patents, Washington, D.C. 20231.

18525-04063

PROVISIONAL APPLICATION COVER SHEET
Additional Page

PTO/SB/16 (10-01)
Approved for use through 10/31/2002 OMB 0651-0032
U.S. Patent and Trademark Office; U.S. DEPARTMENT OF COMMERCE

Under the Paperwork Reduction Act of 1995, no persons are required to respond to a collection of information unless it displays a valid OMB control number

Docket Number		18525-04063
INVENTOR(S)/APPLICANT(S)		
Given Name (first and middle [if any])	Family or Surname	Residence (City and either State or Foreign Country)
Ashraf	Mahmoud	

Number 2 of 2

WARNING: Information on this form may become public. Credit card information should not be included on this form. Provide credit card information and authorization on PTO-2038.

METHOD AND SYSTEM FOR DESIGNING AN IMPROVED ABLATION PATTERN

The methods, systems, and computer readable media described herein relate generally to computer programming and eye surgery and more particularly to designing an ablation pattern for a corneal refractive procedure. The ablation pattern includes an improved transition zone that exhibits continuous curvature between an ablated optical zone and a non-ablated zone, where the effects on vision of ablation in the continuously curved transition zone are accounted for in the ablation pattern design. The continuous curvature in the transition zone facilitates increasing the size of areas that can be ablated to improve vision over conventional methods.

Approximately 60% of Americans have refractive errors, and millions of people are myopic world wide. Thousands of laser refractive surgeries are performed every year for the correction of myopia. Of the many individuals treated, about 15% to 50% do not achieve 20/20 vision due, at least in part, to the relationship of the patient eye to the mean population response eye, the dependence of refractive procedures on the mean population response eye, and ablation patterns that do not take advantage of the widest possible ablation zone. Additionally, many individuals cannot benefit from conventional corneal ablative techniques because their eyes do not fall within parameters modeled by the mean population response eye. For example, using conventional techniques, some corneas are not deep enough for a desired correction.

Conventional ablation algorithms rely on a "black box" approach wherein input variables (e.g., topography measurements) are empirically linked to output variables (e.g., refractive error, visual acuity, glare, aberration, patient satisfaction) in light of the mean population response eye and ablation patterns are designed based on such empirical linking.

Initial attempts at photorefractive keratectomy (PRK) used a model presented in 1988 by Munnerlyn, et al. The cornea was modeled as two refracting surfaces with a bulk material in between the two refracting surfaces where there was a known index of refraction. In treating myopia, the goal was to increase the anterior radius of curvature, thus decreasing the curvature of the anterior surface as illustrated in Figure 1. A simple geometric formula resulted, which assumed the targeted corneal shape was a function of the ablation profile. This is the "shape subtraction" paradigm, based on a geometric approach to tissue removal and secondary curvature change, where the final corneal shape is assumed to be determined

by how much tissue is subtracted by a laser. Essentially, this model treats the cornea as a piece of plastic to be sculpted into an ideal surface shape by laser ablation.

For example, as illustrated in Figs. 1 and 2, for a myopic eye, the cornea is initially "too curved" and thus is conventionally "reshaped" towards a desired "flatter" profile.

5 However, the conventional reshaping in the conventional "optical zone" of a cornea has unanticipated and undesired results. By way of illustration, where the unablated cornea meets the ablated cornea is not smooth, (see Fig. 3) which results in various visual problems including, but not limited to, spherical aberration, glare and halo effects. These effects can be particularly acute in low light conditions when the pupil enlarges. Furthermore, as illustrated
10 in Fig. 4, ablation in the "optical zone", which shallows out the central curvature, has been shown to increase curvature outside the "optical zone", further exacerbating visual problems.

Conventionally, a transition zone is added to an ablation pattern to attempt to smooth out the area between the ablated "correction zone" in the "optical zone" and the non-ablated cornea. Conventionally, this transition zone is not thought to contribute to the corrective
15 effects anticipated as a result of the ablation in the "correction zone" in the "optical zone". For example, a one or two millimeter wide transition zone is added to a conventional (e.g., six millimeter) optical zone for a total ablation pattern of around eight millimeters. But, using a transition zone of continuous curvature, and accounting for its effect on correction, a wider "correction zone" can be designed into ablation patterns. In one example, the
20 correction zone, including both an "optic zone" and a "transition zone" can be up to 10 or 12mm wide.

The conventional transition zone has been added to both regular procedures and "customized" procedures (e.g., those based on topographical and/or wave front analyses). However, such conventional transition zones still have a high curvature that generates a
25 spherical aberration. Furthermore, the corrective effect of the transition zone on vision is not conventionally accounted for in conventional or "customized" procedures.

Both regular conventional procedures and customized conventional procedures are limited by the amount of available cornea to ablate. Conventionally, the wider the optical zone is made, the deeper is the depth of ablation. But, there is a finite amount of corneal
30 depth to ablate, and thus, with conventional patterns, a finite ablatability width. For example, for a desired ten or twelve diopter myopic correction, with a 500 micron thick cornea, conventional patterns may be limited to a 4.5 mm optical zone before running out of ablatability cornea. For a desired correction, 4.5 mm may not be wide enough, and induce glare, and/or

halos and/or spherical aberration. Thus conventional methods may not produce the desired correction. Fig. 15 illustrates two sample depths for two sample optical zone widths.

The equations described by Munnerlyn, et al. still serve as a starting point for ablation algorithms in some conventional treatments for ablation within the optical zone. For a myopic ablation, the pre-operative cornea is modeled as a sphere of greater curvature than the desired post-operative cornea, which is also modeled as a sphere. The apex of the desired post-operative cornea is displaced from the pre-operative cornea by the maximal ablation depth which is determined by the ablation zone size. The intervening tissue is removed or "subtracted" to produce the final result. This is illustrated in Figure 2 for a myopic profile. The Munnerlyn approach, combined with empirical experience, has been relatively successful in correcting spherical and cylindrical errors. However, some patients whose treatment is based on the shape subtraction model do not achieve 20/20 vision. In addition, the shape subtraction model may produce post-operative optical aberrations.

Additionally, wave front guided procedures may also employ a transition zone that may benefit from the systems and methods described herein.

Laser in-situ keratomileusis (LASIK) is also employed to correct vision. LASIK involves cutting a thin corneal flap of tissue, ablating within a stromal bed, and returning the flap. LASIK suffers from drawbacks similar to shape subtraction model PRK, perhaps because these techniques rely on a mean population response, and thus a certain degree of prediction error was inescapable.

When PRK and LASIK failed to consistently produce expected refractive outcomes, it became clear that the model upon which these techniques were predicated was incomplete. Growing appreciation for the complexity of the corneal biomechanical response coupled with a rapidly growing body of clinical experience led to a more empirical approach to algorithm design. Thus, techniques like those described in U.S. Patent No. 5,891,131 titled "Method and Apparatus for Automated Simulation and Design of Corneal Refractive Procedures" issued April 6, 1999 appeared. These techniques attempt to customize a corneal ablation procedure based on the biomechanical response of the cornea to pressure on the cornea.

The cornea has previously been modeled as a biomechanical structure for refractive procedures that do not rely on excimer laser ablation, like radial keratotomy. In these numerical models for refractive surgery, the cornea is assumed to be a solid material and the effect of the surgically induced structural change on cornea deformation produced by an incisional or other procedure, is investigated. The mechanical loading condition employed in

these simulations is the intraocular pressure applied to the posterior surface of the cornea. In techniques like that described in the '131 patent, the biomechanical response of the eye has been incorporated into ablation algorithms. As a result, predictability of the visual result achievable in standard or customized wave front guided or topography guided procedures has been improved. However, there is room for more improvement based on the methods and systems described herein.

In one example, this application concerns designing corneal ablative patterns based on individual biomechanical responses to cutting, ablating and/or peeling a cornea. The corneal ablative pattern includes a wider correction zone that includes both an optical zone and a transition zone, where the transition zone has a continuous curvature and its effects on vision correction are accounted for in the pattern design. The individual biomechanical responses can be predicted from pre-operative measurements and/or from measurements taken during surgery (e.g., after LASIK flap is cut) The individual biomechanical responses can depend on significant differences in the material properties of living human corneas and thus, there are significant differences in the responses of various individuals to similar ablative profiles. Since a flap is cut in a LASIK procedure, the biomechanical responses of the cornea to the cut can be employed to predict a biomechanical response to ablation. Thus, measurements taken before and after cutting the flap facilitate adapting parameters for subsequent ablative steps. The prediction can be facilitated by reference to a biomechanical response model that relates inputs to outputs in light of a plurality of relationships between corneal measurements and individual responses that lead to post ablative corneal shape. In procedures like LASEK and PRK, where no flap is cut, predictions about biomechanical responses can still be made based on pre-operative measurements and a biomechanical response model.

Post-ablative corneal shape, and thus visual performance, is the function of at least three factors: the ablation profile, the healing process, and the biomechanical response of the cornea to structural change. Thus, example biomechanical response models described herein consider these three factors. Furthermore, there are only certain shapes a cornea will biomechanically assume. These shapes depend, at least in part, on epithelial thickness, stromal thickness and response to severing stroma and/or lamellae. For example, the deeper the cut in the edge of the ablation zone in a myopic procedure to generate a potentially desirable post-operative prolate shape, the greater the number of severed lamellae and the greater the biomechanical central flattening response to counter the effect. Thus, example biomechanical response models described herein consider such factors.

LASIK, LASEK, and/or PRK procedures can be improved by taking pre-operative measurements of the eye, predicting the cornea's biomechanical response to ablative treatment, and customizing an ablative pattern design. Parameters considered in customizing the ablation pattern design with an improved transition zone include, but are not limited to, the location, size, shape, depth, and number of cuts and/or ablations. In addition to pre-operative measurements, real time measurements taken during the initial steps of a surgical procedure facilitate analyzing individualized responses and thus in designing a combined ablation zone that includes both an optical zone and an improved transition zone of continuous curvature, and which considers and accounts for the corrective effects of the conventional transition zone. For example, comparison of data including, but not limited to, pre-flap, post-flap, pre-ablation and post-ablation data like corneal thickness, flap thickness, corneal topography, and wave front data provide predictive information applicable to modifying an ablation pattern design.

As used herein, the term "biomechanical response" means a mechanical or physical response to a perturbation or other stimulus (e.g., cutting the cornea, ablating the cornea).

As used in this application, the term "computer component" refers to a computer-related entity, either hardware, firmware, software, a combination thereof, or software in execution. For example, a computer component can be, but is not limited to being, a process running on a processor, a processor, an object, an executable, a thread of execution, a program and a computer. By way of illustration, both an application running on a server and the server can be computer components. One or more computer components can reside within a process and/or thread of execution and a computer component can be localized on one computer and/or distributed between two or more computers.

"Signal", as used herein, includes but is not limited to one or more electrical or optical signals, analog or digital, one or more computer instructions, a bit or bit stream, or the like.

"Software", as used herein, includes but is not limited to, one or more computer readable and/or executable instructions that cause a computer or other electronic device to perform functions, actions and/or behave in a desired manner. The instructions may be embodied in various forms like routines, algorithms, modules, methods, threads, and/or programs. Software may also be implemented in a variety of executable and/or loadable forms including, but not limited to, a stand-alone program, a function call (local and/or remote), a servlet, an applet, instructions stored in a memory, part of an operating system or browser, and the like. It is to be appreciated that the computer readable and/or executable

instructions can be located in one computer component and/or distributed between two or more communicating, co-operating, and/or parallel processing computer components and thus can be loaded and/or executed in serial, parallel, massively parallel and other manners.

The shape subtraction model assumes that the only portion of the cornea that is changed during an ablative procedure is the area within the ablation zone and that even if there are changes outside the ablation zone, they have no effect on central vision. Thus, ablation patterns conventionally do not account for the corrective effect, if any, caused by the changes outside the optical zone. Figure 1 is a schematic of the simple "shape-subtraction" paradigm for correcting myopia. R_1 and R_2 are initial and final radii of curvature, d is the maximum depth of the laser cut, and S is the diameter of the optical zone. Figure 2 is a schematic diagram of the shape-subtraction model of refractive surgery for a myopic ablation. The pre-operative radius of curvature is R_1 and the desired post-operative curvature is R_2 . The maximum ablation depth is determined by the ablation zone size. Thus, conventionally, corrections are limited by the amount and/or character of ablation that can occur within the optical zone. The intervening tissue between the pre-operative curve (solid) and post-operative curve (dashed) is "subtracted" with an excimer laser to produce the desired result. While the shape subtraction model has yielded satisfactory results without considering the biomechanical response of the cornea to perturbation, it can be improved.

Thus, this application concerns application of a biomechanical model of corneal response to laser refractive surgery that considers a plurality of components related to designing an ablation pattern. The components can include ablation profile, laser parameters, epithelial healing, stromal healing, corrective effects of a wider transition zone with continuous curvature, and corneal biomechanical response to a structural change (e.g., cut, ablation). A model based on these components more fully characterizes corneal biomechanical response and thus final corneal shape and facilitates designing an ablation pattern. Thus, existing algorithms and apparatus that produce ablation patterns can be supplemented before and/or during a surgical procedure with individually customized ablation pattern designs to improve resulting vision.

In a myopic procedure, inside the ablation zone, thickness decreases as predicted by the shape subtraction model. However, outside the ablation zone, thickness unexpectedly increases. In addition, regression analysis between the central and peripheral curvature changes shows a negative correlation ($p < 0.0053$), indicating that greater central flattening produces greater peripheral steepening. Elevation and pachymetry maps also show peripheral

increases in both elevation and pachymetry outside the ablation zone, corresponding to the increase in curvature. Once again, the shape subtraction model is found lacking, and thus ablative design patterns based on the shape subtraction model can be improved by considering individual biomechanical response to corneal structural changes and contribution of areas outside the optical zone to central vision.

Altering the corneal structure alters the shape of the entire cornea, whether using an incisional, ablative or thermal mechanism. Fundamentally, if the cornea were a piece of plastic, radial keratotomy would not work. Yet in laser refractive surgery, the structural link between the central and peripheral cornea has not been employed to design ablation patterns. Thus, this application describes systems and methods that consider peripheral stromal thickening or an increase in the corneal elevation outside the optical and/or ablation zone when designing an ablation pattern. Regression analysis between central curvature change and peripheral elevation change from thirty subjects who underwent LASIK procedures demonstrated a positive correlation ($R^2 = 0.56$, $p < 0.0001$) indicating that the greater the increase in elevation outside the ablation zone, the greater the flattening curvature change centrally.

In one case study, regression analysis of central curvature versus peripheral stromal thickness was performed. Central curvature has a negative correlation with peripheral thickness, both inferior and superior, meaning the greater the peripheral thickness, the flatter the central curvature. Thus, the application describes example systems and methods that design ablation patterns with improved transitional zones with continuous curvature based, at least in part, on peripheral stromal thickness.

An example model is presented in Figure 12 that predicts biomechanical central corneal flattening as a direct consequence of severed corneal lamellae. Rather than a piece of plastic, the cornea is modeled as a series of stacked rubber bands (lamellae) with sponges between each layer (interlamellaer spaces filled with ground substance or matrix). The rubber bands bear a tensile load since there is a force pushing on them from underneath (intraocular pressure) and the ends are held tightly by the limbus. The amount of water that each sponge can hold is determined by how tightly the rubber bands are pulled. As the bands are pulled more tightly, the tension in the bands increases and water is squeezed out of the interleaving sponges resulting in smaller, interlamellaer spacing. This is analogous to the pre-operative condition illustrated in Figure 12. After myopic laser refractive surgery, a series of lamellae are severed circumferentially and removed centrally as shown in Figure 12.

The remaining peripheral segments relax just like tight rubber bands would relax once cut. With the reduction of tension in the lamellae, the squeezing force on the matrix is reduced and the distance between lamellae expands due to negative intrastromal fluid pressure. This is analogous to the sponges taking up water if the rubber bands are cut. This allows the periphery of the cornea to thicken. Due to cross linking between the lamellaer layers, the expansion force pulls on the underlying intact lamellae as indicated by the arrows pointing radially outward. An outward force in the periphery pulls laterally on the center and flattens it. Thus, the cornea will flatten centrally with procedures that circumferentially sever lamellae, including hyperopic procedures and therapeutic procedures. The biomechanical flattening enhances a myopic procedure, works against a hyperopic procedure, and causes flattening in a non-refractive PTK. This includes myopic profiles, hyperopic profiles, constant depth PTK profiles, as well as the simple cutting of a LASIK flap. Thus, the example systems and methods described herein rely on the assumption of central corneal flattening and peripheral steepening associated with severing lamellae. By expanding and deepening the transition zone, corneal crosslinks, which are preferentially distributed anteriorly and peripherally, are removed. This should reduce the biomechanical response and allow a more optimal corneal shape to be achieved.

In LASIK procedures, a flap is cut with a microkeratotome to a thickness of approximately 160 microns. Biomechanically, this approximates a 160 micron depth ablation. The amount of corneal flattening produced by the flap cut predicts the biomechanical response of the cornea to ablation. Topography of the epithelial surface of the cornea, before and after cutting the flap, permits real time computation of ablation parameters to account for individual biomechanics with resulting improvements in procedure outcomes. Thus, this application describes systems and methods that compute ablation pattern designs based, at least in part, on corneal measurements taken before and after cutting a LASIK flap.

The cornea has been studied and characterized as a biomechanical entity. The characterizations have included in vitro measurement of material properties like the modulus of elasticity and sheer modulus. Computational models have been generated to approximate the structural response to simulated incisional keratectomy. While these efforts have advanced the basic understanding of corneal behavior under certain specific conditions, the predictive value of existing numerical models is limited by the implicit simplifications of modeling the cornea as a solid substance.

This application describes example systems and methods that rely on biomechanical models of corneal response that consider the lamellaer structure of the corneal stroma and its response to a cut and/or ablation. The stroma dominates the mechanical response of the cornea to injury. The stromal lamellae, by virtue of their extension across the corneal width and continuity with the corneo-scleral limbus, bear a tensile load arising from intraocular pressure and extraocular muscle tension. The propensity of the stroma to imbibe fluid and swell, which is attributed to the hydrophilic macromolecules of the extracellular matrix, is resisted by the corneal limiting layers, the metabolic activity of the corneal endothelium, and the compression effects of lamellaer tension. The thickness of the stroma is linearly related to the hydration and thus is an accessible indicator of changes in corneal mechanical equilibrium. The systems and methods described herein assume that when tension bearing lamellae are disrupted by central or paracentral keratectomy and/or ablation, their peripheral segments relax, causing local decompression of the extracellular matrix and a compensatory influx of stromal fluid adding to increases in interlamellaer spacing and peripheral thickness. Increases in thickness are limited ultimately by interlamellaer cross links, which are distributed in the anterior one third and periphery of the stroma. The example systems and methods described herein further assume that this contributes to regional differences in lamellaer shearing strength and interlamellaer cohesive strength. This assumes that interlamellaer stress generated in the expanding stromal periphery is communicated through this lattice of crosslinks to lamellae that form the post-operative optical surface. Peripheral thickening is assumed to exert an anterolateral tension at the ablation margin and to stimulate central flattening and paracentral changes in shape that contribute to post-operative optical aberrations. Coupling of peripheral and central tensile loads is mediated by interlamellaer cohesive forces distributed in the anterior peripheral stroma. Components of force in the direction of peripheral expansion result in central corneal flattening and peripheral steepening. Thus, by understanding and modeling such responses, improved ablation patterns can be designed where the patterns include a transition zone of continuous curvature that accounts for such peripheral steepening and may reduce it to achieve a more desirable post-operative shape and visual correction.

During procedures like PRK, PTK, LASEK, and LASIK, central ablation causes an immediate circumferential severing of corneal lamellae under tension, with a subsequent relaxation of the corresponding peripheral lamellaer segments. This causes a peripheral decompression of the extracellular matrix and an increase in stromal thickness outside of the

ablation zone. As employed in the example methods and systems described herein, this response is assumed to affect central curvature due partly to the presence of interlamellaer crosslinking, which predominates in the anterior one third and periphery of the stroma and is associated with lamellaer shearing strength and interlamellaer cohesive strength.

5 Interlamellaer stress is generated in the expanding stromal periphery and transferred through this network of crosslinks to the underlying lamellae whose central portions comprise the post-operative anterior surface. The outward expansive force in the periphery causes the central cornea to flatten, independent of the ablation profile. Thus, even in the absence of a myopic (centrally weighted) ablation pattern, biomechanical changes in the cornea can
10 produce an acute post-operative flattening of the central cornea in a refractive shift toward hyperopia. This response is clearly demonstrated by the clinical phenomenon of intended hyperopic shift in PTK. Thus, ablation patterns designed in accordance with this application consider such central corneal flattening and para-central shape changes.

In example models employed by the systems and methods described herein, the
15 stroma, which makes up about 90% of the total corneal thickness, most significantly influences the mechanical response of the cornea to perturbation (e.g., cutting, ablation). The stroma is approximately 78% water by weight, 15% collagen, and 7% other proteins, proteoglycans, and salts. Three hundred to five hundred lamellae, flattened bundles of parallel collagen fibrils, run from limbus to limbus without interruption. In the posterior two
20 thirds of the stroma, the lamellae are successively stacked parallel to the corneal surface so that each lamellae has an angular offset from its anterior and posterior neighbors. Anteriorly, the lamellae are more randomly oriented, often obliquely to the corneal surface, are more branched, and are significantly interwoven. Accounting for the biomechanical response of lamellar severing in the expanded transition zone facilitates improving resulting vision.

25 Cohesive strength is measured as the force required to separate a stromal sample along a cleavage plane parallel to the lamellaer axes by pulling in a direction perpendicular to the cleavage plane similar to peeling a banana as illustrated in Figure 13. Thus, cohesive strength is a measure of the interlamellaer resistance to separation in the transverse direction and is expressed as a function of distance from the corneal center. Alternatively, the shear
30 strength is a resistance to shearing or sliding of one lamellae over another in the plane parallel to the lamellaer axes, the longitudinal direction. Thus, it is an integrated function of the connective forces across the entire lamellaer interface as illustrated in Figure 13. Both forces

contribute to the peripheral to central transfer of stress in a biomechanical response and thus are considered in designing ablation patterns.

In one example, the interlamellaer cohesive strengths of the temporal and nasal peripheries of the horizontal meridian are modeled as being equivalent. The vertical meridian is modeled with consistent differences between the strengths of the superior and inferior regions. In one example, the differences are modeled as a mean central strength of 0.165 ± 0.0088 n/mm and mean peripheral strengths at 4 mm from the central cornea of 0.185 ± 0.0088 n/mm and 0.234 ± 0.0137 n/mm ($p < .01$) for the inferior and superior regions respectively. Furthermore, interlamellaer cohesive strength in the human corneal stroma is modeled as greater in the periphery than in the center. Thus, in one example, the cornea is modeled with an interlamellaer cohesion strength at 50% depth that is greater peripherally than centrally and greater superiorly than inferiorly. Furthermore, based on the predominance of interlamellaer binding in the interior one third of the stroma, the cornea is modeled with magnitudes of forces that are even greater in that region. Thus, in an ablated cornea, a redistribution of tensile loading will induce non-physiological stresses between cut and uncut lamellae.

The lamellaer organization of the stroma and the capacity of this collagenous network to bear tension is a natural starting point for biomechanical models of curvature change. The biomechanics also depend on the relationship between the interfibrillary constituents of the stroma and water, the major component of the stroma. The collagen fibers are enmeshed in a ground matrix of glycosaminoglycans (GAG) like keratan sulfate and chondroitin sulfates of varying degrees of sulfation. Both substances, but particularly chondroitin sulfate, are markedly hydrophilic and contribute to a negative intrastromal fluid pressure under which the entire stroma is heavily compressed. Intraocular pressure further compresses the stroma through its direct effect at the posterior surface and by its contribution to lamellaer tension. The intrastromal pressure, often called the swelling pressure because of its tendency to draw water into the stromal ground substance, has been measured as -50 to -60 mmHg through a variety of in vitro and in vivo techniques.

In the normal physiologic state, this swelling tendency is resisted and relative dehydration is maintained by a combination of lamellaer tension, anterior evaporation of the tear film, low permeability of the epithelial and endothelial layers to water, and active endothelial transport of biocarbonate. During the act of central ablation, however, a number of lamellae proportional to the depth of ablation are obliterated centrally and tension is lost in

their unablated peripheral segments. The resulting loss of compression introduces a hydrostatic disequilibrium, and the peripheral stroma thickens as it takes up fluid. The swelling pressure diminishes as stromal hydration and thickness increase and a new steady state is established.

5 A link exists between peripheral stromal thickening and central flattening based on a mechanical relationship between disrupted and intact lamellae. This is contrary to previous models where lamellae are assumed to be structurally and mechanically independent of neighboring lamellae, that is, arranged in layers without interconnections. In previous models, the tensile load previously borne by the full complement of lamellae is shifted to the
10 remaining posterior fibers, which now strain (stretch) slightly under the concentrated stress. If the limbal circumference is assumed to be fixed, the stretch may not be accomplished by an increase in corneal diameter and must therefore occur as central corneal bulging and anterior steepening. However, if the proposed peripheral response is considered, this occurs as a peripheral thickening and peripheral steepening with coincident central flattening. Although
15 previous models describe the characteristic peripheral "knee" and central flat zone of PTK, PRK, and LASIK, finite element analyses of uniform thickness profiles have not incorporated the peripheral response and have predicted a corneal configuration opposite that produced clinically. Thus, consideration of the proposed peripheral stromal response and its mechanical relationship to the central cornea, as well as the negative intrastromal pressure is
20 employed in systems, methods, and based models described herein for more correctly predicting the magnitude and/or direction of refractive correction and thus for designing ablation patterns with improved optical and transitional zones.

 The systems and methods described herein assume that shape changes measured outside an optical zone and/or ablation zone can affect curvature changes within an optical
25 and/or ablation zone. Central curvature change in refractive surgery is not solely a product of the optical zone design pattern. When peripheral thickness and ablation zone bias are included in a regression model, over 83% of the variance and curvature response is explained by peripheral thickening. Thus, a biomechanical response considered herein assumes additional flattening over and above conventionally programmed ablation profiles. This
30 occurs in both myopic (with an intent to flatten), hyperopic (with an attempt to steepen), and/or non-refractive PTK.

 In LASIK surgery, cutting the flap alters the corneal structure. Corneal measurements taken following the cutting of the corneal flap are therefore employed by example methods

and systems described herein. The microkeratomic incision for the flap produces changes in the cornea. The redistribution of strain caused by the keratomic incision causes the central cornea to flatten and the peripheral stroma matrix to thicken and become steeper. This reshaping assists with a central myopic correction, where decreased corneal curvature is prescribed, and works against a hyperopic correction where increased corneal curvature is prescribed. Since cutting the LASIK flap produces a biomechanical response, a method for customizing a refractive ophthalmic treatment by designing the ablation pattern with an improved optical zone plus transitional zone can include pre-operatively measuring the cornea, cutting the flap, measuring the cornea and/or the flap, designing the ablation pattern, and performing a customized ablation based on the pattern.

In LASEK and PRK surgery, no flap is cut. However, based on pre-operative measurements, with reference to a biomechanical response model, an ablation pattern with an improved optical zone plus transition zone can similarly be designed.

In an example method, corneal measurements are taken by methods including, but not limited to, corneal topography, optical coherence tomography, ultrasound, refraction, and/or wave front analysis. In LASIK, these measurements are taken before and after the microkeratomic incision for the corneal flap. In LASEK and PRK, the measurements are only taken before the procedure. In LASIK, differences in corneal measurements can be compared to expected and achieved post-cut results. Comparison of the measurements before and after the incision facilitate adjusting an ablative pattern design to account for the measured biomechanical response due to the cutting, and the predicted biomechanical response anticipated through the ablation. Ablation pattern adjustments can thus be made in advance of the ablation in a separate procedure and/or in real time as an intraoperative adjustment after the perturbation (e.g., cut, ablation) but before the ablation.

Optimal surgical procedures benefit from considering the biomechanical results of the ablative procedure itself. Thus, an example LASIK surgical technique employing the systems and methods described herein includes, but is not limited to, accessing a model of predicted responses based on empirical data collected from corneas before and after cutting a flap, ablation, and healing. The technique further includes taking pre-perturbation measurements (e.g., thickness profile, curvature profile, corneal size) and employing these measurements in connection with the model to facilitate computing ablation pattern designs. The method further includes taking post perturbation measurements (e.g., thickness profile, curvature profile, central flattening, peripheral thickening), and employing these

measurements to compute one or more ablation parameters. A sample LASEK or PRK surgical technique would only acquire pre-operative data that can be employed to query the biomechanical response model. The technique further includes comparing the differences between the pre-perturbation measurements and the post perturbation measurements to facilitate refining the computed ablation parameters and/or the model.

Example biomechanical response models can also consider Young's modulus measurements, and other factors including, but not limited to, age, sex, race, years of contact lens wear, thickness, curvature, and corneal size. While data concerning some factors are acquired by measuring, other data can be acquired during a patient interview (e.g., years of contact lens use). Measurements of one or more of these factors facilitate selecting which pre-operative parameters to employ to predict a biomechanical response. Thus, ablation patterns may be designed based on pre-operative data.

Pre-operative and postoperative measurements can be input to one or more computer components by methods including, but not limited to, key stroke, direct data transfer, and so on. During cornea surgery, the methods described herein may be performed on a computer system with which a surgical team member communicates. Data may be input to the computer during the surgical process. The method can then produce data, such as ablation parameters, that can be employed in subsequent steps of the surgery.

In view of the exemplary systems shown and described herein, example methodologies that are implemented will be better appreciated with reference to the flow diagrams of Figures 9 and 11. While for purposes of simplicity of explanation, the illustrated methodologies are shown and described as a series of blocks, it is to be appreciated that the methodologies are not limited by the order of the blocks, as some blocks can occur in different orders and/or concurrently with other blocks from that shown and described. Moreover, less than all the illustrated blocks may be required to implement an example methodology. Furthermore, additional and/or alternative methodologies can employ additional, not illustrated blocks. In one example, methodologies are implemented as computer executable instructions and/or operations, stored on computer readable media including, but not limited to an application specific integrated circuit (ASIC), a compact disc (CD), a digital versatile disk (DVD), a random access memory (RAM), a read only memory (ROM), a programmable read only memory (PROM), an electronically erasable programmable read only memory (EEPROM), a disk, a carrier wave, and a memory stick.

In the flow diagrams, rectangular blocks denote "processing blocks" that may be implemented, for example, in software. Similarly, the diamond shaped blocks denote "decision blocks" or "flow control blocks" that may also be implemented, for example, in software. Alternatively, and/or additionally, the processing and decision blocks can be implemented in functionally equivalent circuits like a digital signal processor (DSP), an application specific integrated circuit (ASIC), and the like.

A flow diagram does not depict syntax for any particular programming language, methodology, or style (e.g., procedural, object-oriented). Rather, a flow diagram illustrates functional information one skilled in the art may employ to program software, design circuits, and so on. It is to be appreciated that in some examples, program elements like temporary variables, routine loops, and so on are not shown.

Turning now to Figure 9, a flow chart illustrates an example method 900 that facilitates customizing refractive ophthalmic treatment by designing a custom ablation pattern that includes a wider ablation zone including an optical zone and a transition zone of continuous curvature, where the corrective properties of the transition zone are included in the design. At 910, a corneal biomechanical response model is accessed. For example, one or more records, tables, fields, procedure calls, objects, pieces of data and so on may be retrieved. At 920, the method 900 receives a pre-perturbation data concerning a cornea on which a refractive ophthalmic treatment will be performed. The pre-perturbation data can include, but is not limited to, a topographic data, a pachymetric data, an elevation data, a corneal thickness data, a corneal curvature data, a wave front data, and an intraocular pressure data, where such data are associated with the cornea before it has been perturbed. The perturbation can be one of a corneal incision, a corneal ablation, a LASIK flap cut, and peeling the epithelial layer from the cornea, for example.

At 930, the method 900 receives a post perturbation data. The post perturbation data can include, but is not limited to, a topographic data, a pachymetric data, an elevation data, a total corneal thickness data, a corneal curvature data, a wave front data, a flap thickness data, and an intraocular pressure data. The perturbation can be, for example, a corneal incision, a corneal ablation, a LASIK flap cut, and an epithelial layer peel.

At 940, based, at least in part, on the pre-perturbation data received at 920 and the post perturbation data received at 930, the method 900 designs ablation pattern with an improved transition zone whose corrective effects are accounted for. The ablation pattern may be designed in accordance with a biomechanical response modeled in a biomechanical

response model accessed at 910. In one example, the biomechanical response model predicts the biomechanical response, at least in part, by considering the impact of severing corneal lamellae during the perturbation.

In an extension of method 900 (not illustrated), additional processing is undertaken.

5 This additional processing includes receiving a post-operative diagnosis data and selectively updating the biomechanical response model based, at least in part, on the post-perturbation data and/or the post-operative diagnosis data. In this way, the predictive biomechanical response model can be updated over time to become more complete and thus provide even more accurate predictions and thus better designs. The post-operative diagnosis data can

10 include, but is not limited to, a patient satisfaction data, a patient vision data, a patient halo effect data, a topographic data, a pachymetric data, an elevation data, a total corneal thickness data, a corneal curvature data, a wave front data, and an intraocular pressure data.

In an alternate implementation of method 900 (not illustrated), no LASIK flap is cut, and thus no post-perturbation data is acquired. The improved ablation pattern is designed

15 from pre-operative measurements and with reference to a biomechanical response model.

Turning now to Figure 10, a system 1000 for designing an ablation pattern is illustrated. The system 1000 includes a data receiver 1010 that receives a corneal data 1020. The corneal data can include, but is not limited to, a topographic data, a pachymetric data, an elevation data, a total corneal thickness data, a corneal curvature data, a wave front data, and

20 an intraocular pressure data measured before and/or after a cornea is processed by at least one of a cut, an ablation, and an epithelial peel. In LASEK and PRK, the corneal data will not include post-perturbation data, with the design being based on pre-operative measurements with reference to the biomechanical response model.

The system 1000 also includes a predictive corneal biomechanical response model

25 1030. The predictive corneal biomechanical response model 1030 facilitates designing ablation patterns based on the corneal data 1020. Thus, the system 1000 includes an ablation pattern designer 1040 that designs a refractive ophthalmic ablation pattern 1050. The predictive corneal biomechanical response model 1030 can include components like a peripheral stromal thickening analyzer, a corneal elevation analyzer, a position dependent

30 negative pressure analyzer, a corneal lamellae severing analyzer, an acute depth response analyzer, and so on. The pattern designer 1040 produces a pattern that is wider (e.g., 10-12 mm) than is possible with conventional systems (e.g., 4-6 mm) and includes a transition zone of continuous curvature whose corrective effects are accounted for in the design.

Turning now to Figure 11 , an example method 1100 for a corneal ablative surgical method is illustrated. At 1110, a first set of corneal measurements are taken. These measurements are taken before corneal lamellae are severed. At 1120, one or more severing parameters are selected by the person and/or machine performing the corneal ablative surgical method 1100. These severing parameters are based, at least in part, on the first set of corneal measurements. For example, a corneal topography measurement may indicate that a certain severing depth should be attempted in the corneal ablative surgical method. Similarly, a pachymetric data may indicate that a certain severing location should be selected.

At 1130, one or more corneal lamellae are severed. It is to be appreciated that this severing can be accomplished by techniques including, but not limited to, an incision and an ablation.

At 1140, a second set of corneal measurements are taken after the one or more corneal lamellae are severed. At 1150, based on the first corneal measurements, and/or the second corneal measurements, an ablation pattern can be designed. The design will include a wider ablation zone and an improved transition zone that contributes to correction and whose contribution is considered.

At 1160, based at least in part on the ablation parameters selected at 1150, corneal tissue is ablated from a cornea.

Those skilled in the art of computer programming, mathematical computer modeling, and/or data base manipulation and administration will readily appreciate that example systems and methods described herein may be embodied in software and/or one or more computer components. Thus, Figure 14 illustrates a computer 1400 that includes a processor 1402, a memory 1404, a disk 1406, input/output ports 1410, and a network interface 1412 operably connected by a bus 1408. Executable components of systems described herein may be located on a computer like computer 1400. Similarly, computer executable methods described herein may be performed on a computer like computer 1400. It is to be appreciated that other computers may also be employed with the systems and methods described herein. The processor 1402 can be a variety of various processors including dual microprocessor and other multi-processor architectures. The memory 1404 can include volatile memory and/or non-volatile memory. The non-volatile memory can include, but is not limited to, read only memory (ROM), programmable read only memory (PROM), electrically programmable read only memory (EPROM), electrically erasable programmable read only memory (EEPROM), and the like. Volatile memory can include, for example, random access memory (RAM),

synchronous RAM (SRAM), dynamic RAM (DRAM), synchronous DRAM (SDRAM), double data rate SDRAM (DDR SDRAM), and direct RAM bus RAM (DRRAM). The disk 1406 can include, but is not limited to, devices like a magnetic disk drive, a floppy disk drive, a tape drive, a Zip drive, a flash memory card, and/or a memory stick. Furthermore, the disk 1406 can include optical drives like, compact disk ROM (CD-ROM), a CD recordable drive (CD-R drive), a CD rewriteable drive (CD-RW drive) and/or a digital versatile ROM drive (DVD ROM). The memory 1404 can store processes 1414 and/or data 1416, for example. The disk 1406 and/or memory 1404 can store an operating system that controls and allocates resources of the computer 1400.

10 The bus 1408 can be a single internal bus interconnect architecture and/or other bus architectures. The bus 1408 can be of a variety of types including, but not limited to, a memory bus or memory controller, a peripheral bus or external bus, and/or a local bus. The local bus can be of varieties including, but not limited to, an industrial standard architecture (ISA) bus, a microchannel architecture (MSA) bus, an extended ISA (EISA) bus, a peripheral component interconnect (PCI) bus, a universal serial (USB) bus, and a small computer systems interface (SCSI) bus.

15 The computer 1400 interacts with input/output devices 1418 via input/output ports 1410. Input/output devices 1418 can include, but are not limited to, a keyboard, a microphone, a pointing and selection device, cameras, video cards, displays, and the like. 20 The input/output ports 1410 can include but are not limited to, serial ports, parallel ports, and USB ports.

25 The computer 1400 can operate in a network environment and thus is connected to a network 1420 by a network interface 1412. Through the network 1420, the computer 1400 may be logically connected to a remote computer 1422. The network 1420 includes, but is not limited to, local area networks (LAN), wide area networks (WAN), and other networks. The network interface 1412 can connect to local area network technologies including, but not limited to, fiber distributed data interface (FDDI), copper distributed data interface (CDDI), ethernet/IEEE 802.3, token ring/IEEE 802.5, and the like. Similarly, the network interface 1412 can connect to wide area network technologies including, but not limited to, point to point links, and circuit switching networks like integrated services digital networks (ISDN), packet switching networks, and digital subscriber lines (DSL).

30 Turning now to Fig. 16, a tangential map and a refractive power map associated with a pre-operative cornea are illustrated. On the tangential map warmer colors (e.g., yellow,

red) represent more curved areas. On the refractive map, the warmer colors represent areas of greater power. Conversely, cooler colors (blue, purple) represent areas of lesser curvature on the tangential map, and lower power on the refractive map. Thus, in Fig. 16, the tangential map illustrates that the cornea is steeper in the middle and flatter in the periphery. The refractive power map illustrates that power increases as you move from the center of the cornea to the edge of the cornea.

Figure 17 illustrates a tangential map and a refractive power map for a post-operative cornea, where the cornea was ablated using a conventional transition zone and ablation algorithm. The tangential map illustrates the central flattening as compared to the pre-operative cornea and the characteristic red ring that indicates a very steep area caused by a sub-optimal transition zone design. The refractive power map has a characteristically small central blue area that can be improved using the systems and methods described herein.

Figure 18 illustrates a tangential map and a refractive power map for a post-operative cornea, where the cornea was ablated using the transition zone and ablation algorithms described herein. The tangential map illustrates the central flattening as compared to the pre-operative cornea but the red ring has been moved farther away from the center of the cornea. This facilitates mitigating problems associated with spherical aberration. Also, by moving the transition zone, a larger area of improved curvature can be achieved. For example, in the refractive power map, the central blue area is much larger, indicating a larger, more useful area of corrected vision, with fewer effects of spherical aberration.

In both figures 17 and 18, the post operative corneas had substantially the same optical zone size where Munnerlyn correction formulae were applied. However, with the improved transition zone and improved ablation algorithm, a larger, better designed transition zone moved the red ring out, improving vision and mitigating the effects of spherical aberration.

The systems, methods, data structures, models and objects described herein may be stored, for example, on a computer readable media. Media can include, but are not limited to, an application specific integrated circuit (ASIC), a compact disc (CD), a digital versatile disk (DVD), a random access memory (RAM), a read only memory (ROM), a programmable read only memory (PROM), a disk, a carrier wave, a memory stick, and the like.

What has been described above includes several examples. It is, of course, not possible to describe every conceivable combination of components or methodologies for purposes of describing the methods, systems, computer readable media and so on employed

in improving the computation of ablation parameters. However, one of ordinary skill in the art may recognize that further combinations and permutations are possible. Accordingly, this application is intended to embrace alterations, modifications, and variations that fall within the scope of the appended claims. Furthermore, to the extent that the term "includes" is
5 employed in the detailed description or the claims, it is intended to be inclusive in a manner similar to the term "comprising" as that term is interpreted when employed as a transitional word in a claim.

Brief Description of the Drawings

Figure 1 illustrates a shape subtraction model.

Figure 2 illustrates a shape subtraction model of refractive surgery for myopic ablation.

5 Figure 3 illustrates a non-smooth transition between an ablated area and a non-ablated area.

Figure 4 illustrates a non-smooth transition between an ablated area and a non-ablated area, where the transition zone is affected by peripheral corneal steepening after central ablation.

10 Figure 5 illustrates a shape subtraction model of refractive surgery for a hyperopic ablation.

Figure 6 illustrates a non-smooth transition between an ablated area and a non-ablated area.

15 Figure 7 illustrates an improved optical zone that includes both a conventional optical zone and a conventional transition zone whose contribution to optical correction is considered.

Figure 8 illustrates a smoothed transition zone whose corrective effect is accounted for in an ablation pattern.

Figure 9 is a flow chart of an example method for designing an ablation pattern.

20 Figure 10 is a schematic block diagram of an example system for designing an ablation pattern.

Figure 11 is a flow chart of an example corneal ablative surgical method.

Figure 12 illustrates a conceptual model for predicting biomechanical central flattening as a consequence of severing corneal lamellae.

25 Figure 13 is a schematic diagram of example forces described by (A) interlamellar cohesive strength and (B) interlamellar shear strength.
porous material model.

Figure 14 is a schematic block diagram of an example computing environment that supports the methods and systems described herein.

30 Figure 15 illustrates two different ablation widths and the corresponding ablation depths.

Figure 16 illustrates a tangential map and a refractive power map for a cornea before ablative surgery.

Figure 17 illustrates a tangential map and a refractive power map for a cornea following a conventional ablative procedure.

Figure 18 illustrates a tangential map and a refractive power map for a cornea following an ablative procedure that employs the systems and methods described herein for
5 an improved transition zone.

Claims

What is claimed is:

1. A computer implemented method for designing a refractive ophthalmic ablation pattern with an improved ablation zone comprising an optical zone and a transition zone of continuous curvature, comprising:
 - accessing a corneal biomechanical response model;
 - receiving a pre-perturbation data concerning a cornea on which a refractive ophthalmic treatment will be performed;
 - receiving a post-perturbation data concerning the cornea on which the refractive ophthalmic treatment will be performed; and
 - designing a refractive ophthalmic ablation pattern based, at least in part, on at least one of the pre-perturbation data, the post-perturbation data, and the corneal biomechanical response model.
2. The method of claim 1, where the perturbation is one of a corneal incision, a corneal ablation, a LASIK flap cut, and peeling a corneal epithelium.
3. The method of claim 2, where the pre-perturbation data comprises at least one of a topographic data, a pachymetric data, an elevation data, a total corneal thickness data, a corneal curvature data, a wave front data, and an intraocular pressure data.
4. The method of claim 2, where the post-perturbation data comprises at least one of a topographic data, a pachymetric data, an elevation data, a total corneal thickness data, a corneal curvature data, a wave front data, a flap thickness data, and an intraocular pressure data.
5. The method of claim 2, where the corneal biomechanical response model predicts a biomechanical response of a cornea to the refractive ophthalmic treatment.
6. The method of claim 5, where the biomechanical response is predicted by computing the impact of severing corneal lamellae.

7. A computer readable medium storing computer executable instructions operable to perform the method of claim 1.
8. A system for designing an ablation pattern, comprising:
5 a data receiver for receiving a corneal data;
a predictive corneal biomechanical response model; and
an ablation pattern designer for designing the ablation pattern based, at least in part, on the corneal data and the predictive corneal biomechanical response model, where the ablation pattern includes both an ablated optic zone and an ablated transition zone of
10 continuous curvature, where the corrective effect of the transition zone is considered in the design.
9. The system of claim 8, where the corneal data comprises at least one of a topographic data, a pachymetric data, an elevation data, a total corneal thickness data, a corneal curvature
15 data, a wave front data, and an intraocular pressure data measured before a cornea is processed by at least one of a cut, an ablation, and a peeling of a corneal epithelial layer.
10. The system of claim 9, where the corneal data comprises at least one of a topographic data, a pachymetric data, an elevation data, a total corneal thickness data, a corneal curvature
20 data, a wave front data, a flap thickness data, and an intraocular pressure data measured after a cornea is processed by at least one of a cut, an ablation, and a peeling of a corneal epithelial layer.
11. The system of claim 8, where the predictive corneal biomechanical response model
25 comprises at least one of:
a peripheral stromal thickening analyzer;
a corneal elevation analyzer;
a position dependent negative pressure analyzer;
a corneal lamellae severing analyzer; and
30 an acute depth response analyzer.
12. A computer readable medium storing computer executable components of the system of claim 8.

**This Page is Inserted by IFW Indexing and Scanning
Operations and is not part of the Official Record**

BEST AVAILABLE IMAGES

Defective images within this document are accurate representations of the original documents submitted by the applicant.

Defects in the images include but are not limited to the items checked:

- ☐ BLACK BORDERS
- ☐ IMAGE CUT OFF AT TOP, BOTTOM OR SIDES
- ☐ FADED TEXT OR DRAWING
- ☐ BLURRED OR ILLEGIBLE TEXT OR DRAWING
- ☐ SKEWED/SLANTED IMAGES
- ☐ COLOR OR BLACK AND WHITE PHOTOGRAPHS
- ☐ GRAY SCALE DOCUMENTS
- ☐ LINES OR MARKS ON ORIGINAL DOCUMENT
- ☒ REFERENCE(S) OR EXHIBIT(S) SUBMITTED ARE POOR QUALITY
- ☐ OTHER: _____

IMAGES ARE BEST AVAILABLE COPY.

As rescanning these documents will not correct the image problems checked, please do not report these problems to the IFW Image Problem Mailbox.